

Supporting Information.

Metal Acetylacetonate – Bidentate Ligand Interaction (MABLI) as Highly

Efficient Free Radical Generating Systems for Polymer Synthesis

P. Garra¹, F. Morlet-Savary¹, B. Graff¹, F. Dumur², Valérie Monnier³, C. Dietlin¹, D. Gigmes²
J.P. Fouassier, J. Lalevée¹

¹Institut de Science des Matériaux de Mulhouse IS2M, UMR CNRS 7361, UHA; 15, rue Jean Starcky, 68057 Mulhouse Cedex, France

² Aix Marseille Univ, CNRS, ICR UMR 7273, F-13397 Marseille, France.

³ Aix-Marseille Univ, Spectropole, F-13397 Marseille, France

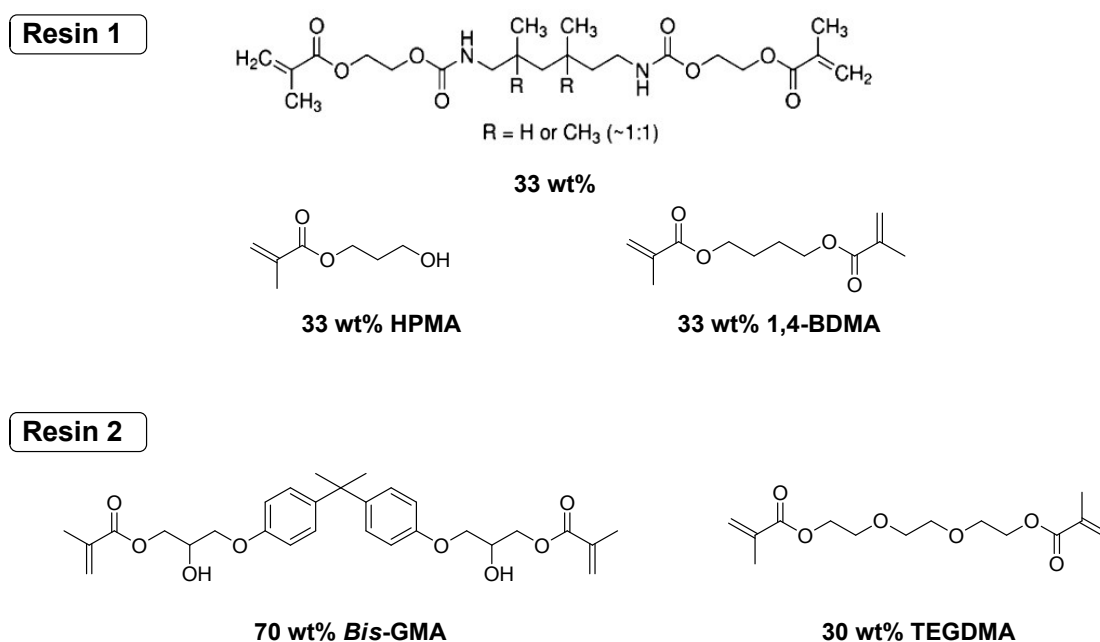
Experimental section

a/ Chemical compounds

All the reactants were used as received. *N*-tert-butyl- α -phenyl-nitrone (PBN), 4-hydroxy-TEMPO (tempol), 2-diphenylphosphinobenzoic acid (2dppba), 4-diphenylphosphino benzoic acid (4dppba), 4-*N,N* trimethylaniline (4-*N,N* TMA), *tris*(2,2,6,6-tetramethyl-3,5-heptanedionato) manganese(III) (Mn(tBuacac)₃), tin(IV) *bis*(acetylacetonate) dichloride (Sn(acac)₂(Cl)₂), manganese acetylacetonate (Mn(acac)₃), copper acetylacetonate (Cu(acac)₂), dibenzoyl peroxide (BPO), ruthenium acetylacetonate (Ru(acac)₃), iron(III) acetylacetonate (Fe(acac)₃), cobalt acetylacetonate (Co(acac)₂), titanium oxide acetylacetonate (Ti(O)(acac)₂), zinc acetylacetonate hydrate (Zn(acac)₂), manganese acetate hydrate (Mn(OAc)₃), 2-bromoacetophenone (Br_Bz), magnesium acetylacetonate((Mg(acac)₂), copper acetate (Cu(OAc)₂)chromium acetylacetonate (Cr(acac)₃), zirconium acetylacetonate (Zr(acac)₄), gallium acetylacetonate (Ga(acac)₃), ethylenediaminetetraacetic acid (EDTA), triphenylphosphine (TPP), citric acid (Ci Ac), ascorbic acid (As Ac), acetic acid (Acet Ac), tert-Butyl perbenzoate (tBu-PBZ), cumene hydroperoxide (CumOOH) and (1R,2R)-(+)-1,2-Diaminocyclohexane-*N,N'*-bis(2-diphenylphosphinobenzoyl) (trost) were purchased from Sigma-Aldrich. Silver acetylacetonate (Ag(acac)), palladium acetylacetonate (Pd(acac)₂), nickel (II) 2,4-pentanedionate (Ni(acac)₂), 2-diphenylphosphinonaphthoic acid (2dppna),

vanadium acetylacetonate ($V(acac)_3$) were obtained from Alfa Aesar. Vanadyl acetylacetonate ($V(O)(acac)_2$), (Oxydi-2,1-phenylene)bis(diphenylphosphine) (DPEphos), 2-(Diphenylphosphino)benzotrile (2dpCN) were purchased from Tokyo chemical industry (TCI). Acetonitrile (ACN) and toluene were obtained from Carlo Erba. 2 diphenylamino benzoic acid (2dpnba) was obtained from Molport.

Copper (II) benzylacetonate ($Cu(Bzacac)_2$) was synthesized according to a procedure found in the literature¹⁻³.



Scheme S1. Main composition of the model methacrylate resins (resin 1 and resin 2).

The efficiency of the different radical generating systems was checked through polymerization in two methacrylate based formulations. The first methacrylate resin noted resin 1 with a low viscosity of 0.053 Pa.s (Figure S1) consists in 1/3 (w/w) 1,4-butanediol-dimethacrylate, 1/3 (w/w) hydroxypropylmethacrylate (HPMA) and 1/3 (w/w) of a representative urethane-dimethacrylate (all obtained from Sigma Aldrich). The second methacrylate blend, noted resin 2 (Figure S1) is composed of a BisGMA/TEGDMA (30/70 wt%) blend having a much higher viscosity (5.7 Pa.s) than resin 1⁴.

All formulations were prepared from the bulk resins in two separate cartridges at room temperature (RT) ($22 \pm 1^\circ\text{C}$) under air: a first component containing the oxidizing agents or metal acetylacetonate and another component containing the phosphine and/or reducing agent. A 1:1 Sulzer mixpac[®] mixer was used to mix both components together at the beginning of each polymerization experiment ($t=0$ sec).

b/ Bulk polymerization followed by optical pyrometry

The use of optical pyrometry to follow photopolymerization reactions was developed by Crivello et al.^{5,6} A rather similar setup was used here: temperature versus time profiles were also followed using an Omega OS552-V1-6 Industrial Infrared Thermometer (Omega Engineering[®], Inc., Stamford, CT) having a sensitivity of $\pm 1^\circ\text{C}$ for 2 g (sample thickness ~ 4 mm). All polymerizations were carried out under air (Surface diameter= 25 mm).

c/ Surface analysis (z-profile) through Raman confocal microscopy

Raman spectra of cured polymer surfaces were recorded with a Labram (Horiba) spectrometer mounted on an Olympus BX40 confocal microscope, operating at 632.8 nm with a 1800 line/mm grating. Carbonyl peak area (1690 to 1755 cm^{-1}) was measured as an internal standard while the alkene peak area (1630 to 1660 cm^{-1}) was used to determine the C=C conversion. Spectra were recorded onto uncured monomer to be used as references for double bond conversion. A 100 \times objective was used in combination with a confocal hole aperture of 200 μm giving an axial resolution of 2.3 μm . Objective displacement in the air was multiplied by a factor of 1.7 following a protocol available in the literature⁷⁻¹¹ to access the “real” depth in the polymerized sample considering a refraction index close to 1.5.

d/ UV-visible absorption spectroscopy

A Varian[®] Cary 3 spectrophotometer was used for recording the UV-vis absorption spectra in ACN during $\text{Mn}(\text{acac})_3$ change of ligand.

e/ Electron Spin Resonance (ESR) – ESR Spin Trapping (ESR – ST)

Electron spin resonance experiments were carried out using a X-band spectrometer (Bruker EMX-plus Biospin). The radicals were observed at room temperature under air in toluene solution. Since the acac• radical exhibits a short lifetime, ESR-ST experiments were realized using PBN as a spin trapping agent in a similar way as described in other works¹². ESR spectra simulations were carried out using the WINSIM software.

f/ High Resolution ElectroSpray Ionization – Mass spectrometry (HR-ESI-MS)

HR-ESI-MS was performed using a SYNAPT G2 HDMS (Waters). 2 samples were analyzed in 300 μ L dichloromethane (Aldrich): first, 5.2 mg Mn(acac)₃ was mixed with 2 eq 2dppba; next, 3.5 mg V(O)(acac)₂ + 10 eq 2dppba. These two solutions were diluted at 1/10 in a methanol solution containing 3 mM ammonium acetate. They were subsequently introduced in the ionization source at a flow rate of 10 μ L/min. Commercial polyethylene glycol (PEG400) was used as an internal standard. (see detailed replicates in Table S5).

g/ Cyclic Voltammetry (CV)

The reduction potential (E_{red} vs. SCE) and oxidation potential (E_{ox} vs. SCE) of the studied compound was determined by cyclic voltammetry (Voltalab PST006) in acetonitrile solution containing tetrabutylammonium hexafluorophosphate (Aldrich) as the supporting electrolyte. A platinum electrode was used as a working electrode and a saturated calomel electrode (SCE) was used as a reference electrode.

h) Nuclear Magnetic Resonance (¹H and ³¹P NMR)

Nuclear Magnetic Resonance (¹H and ³¹P NMR) were recorded in CDCl₃ solution on a 300 MHz Varian Mercury spectrometer.

i) Computational Procedure

Enthalpies of Reactions for each metal acetylacetonate – 2dppba reaction were calculated with the Gaussian 03 package. Geometries optimization¹³ were calculated at UB3LYP/LANL2DZ level; geometries were frequency checked. Formation enthalpy of each product was subtracted by formation enthalpy of each reagent in r1 to obtain enthalpy of MABLI reaction. Visualizations of the optimized geometries are available in Supplementary information.

Supplementary results

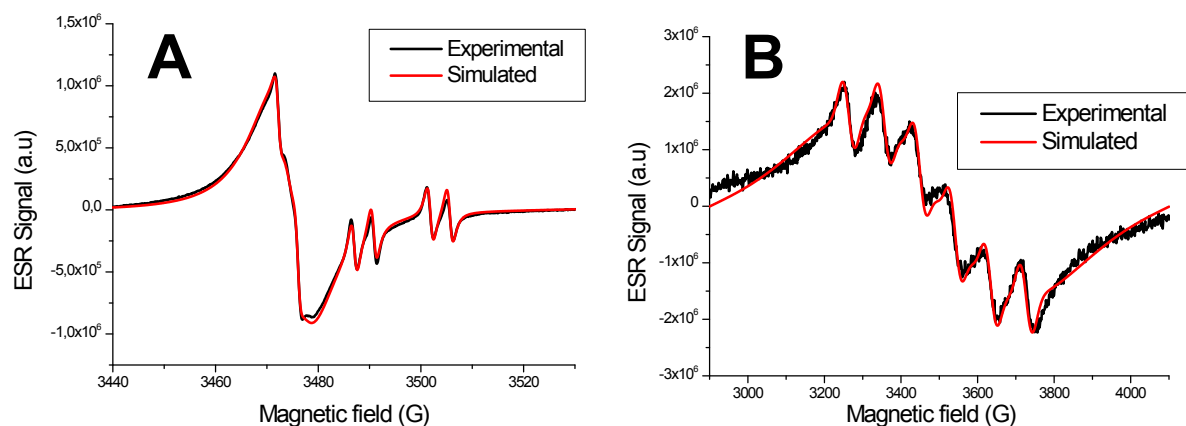
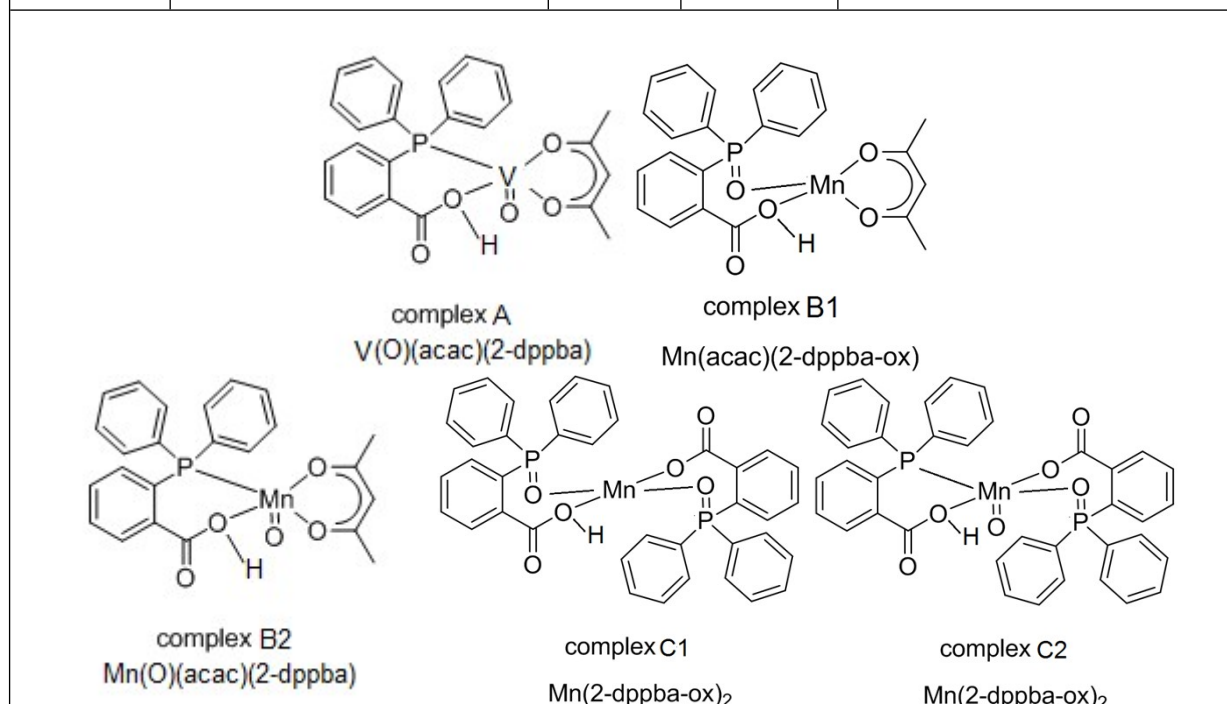


Figure S1: ESR spectra in toluene/DCM (90/10 v/v) under air, at room temperature. **A:** (-) 2.4 mM $V(acac)_3$ mixed with 8 eq 2dppba in the presence of PBN spin trapping agent (-) simulated spectra ($a_N = 14.80$ G and $a_H = 3.80$ G). **B:** (-) 0.44 mM $Mn(acac)_3$ mixed with 2.35 eq 2dppba. (-) simulated spectra (first specie: $a_{Mn} = 92$ G ; spin of Mn: 5/2 and a second specie: powder broad signal)

Table S1: HR-ESI-MS data and proposed structural interpretation of the different adduct of the MABLI process. For two ligand exchanges: experiment 1: $V(O)(acac)_2 + 10 \text{ eq } 2dppba$ and experiment 2: $Mn(acac)_3 + 2 \text{ eq } 2dppba$.

Experiment	Detected (HR-ESI-MS) $[M+H]^+$	m/z (Da)	Error	Proposed attribution
1	$C_{24}H_{22}O_5PV$	472.0639	< 2 ppm	complex A
2	$C_{24}H_{22}O_5PMn$	476.0580	< 3 ppm	complex B1 or B2
2	$C_{38}H_{29}O_6P_2Mn$	698.0814	< 2 ppm	complex C1 or C2



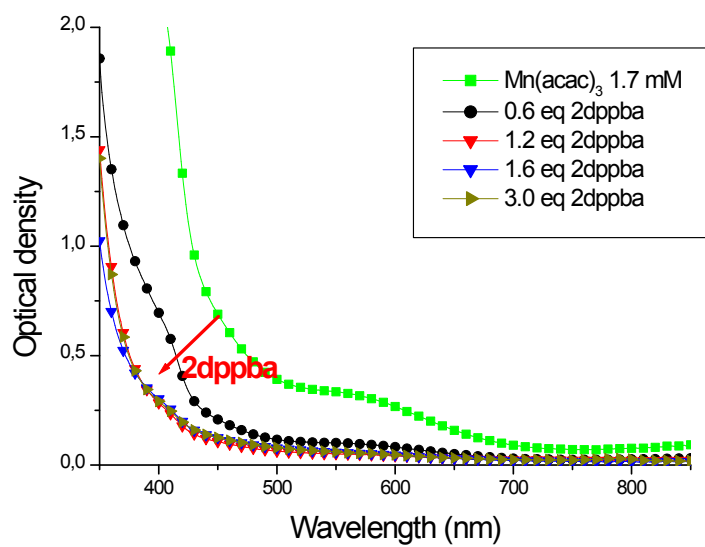


Figure S2: Study of the **Stoichiometry** of the ligand exchange using UV-Vis spectrometry in propan-2-ol; Initial concentration of Mn(acac)₃ = 1.7mM and increasing concentration of 2dppba

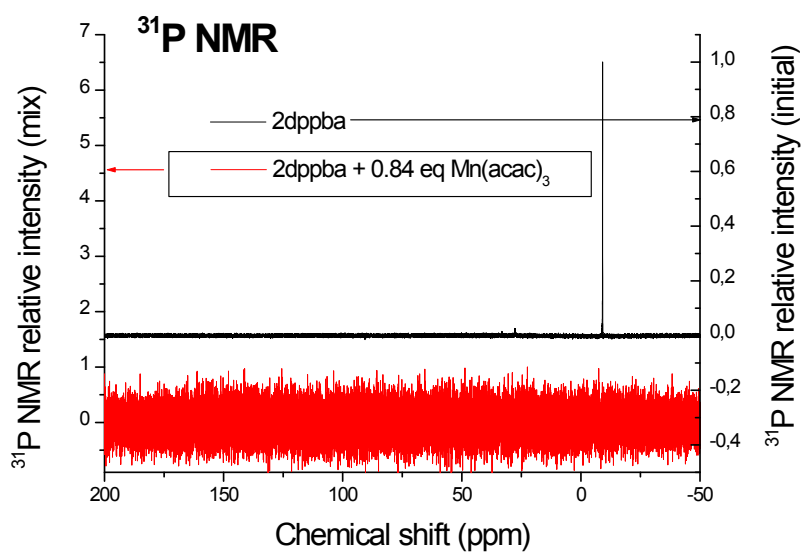
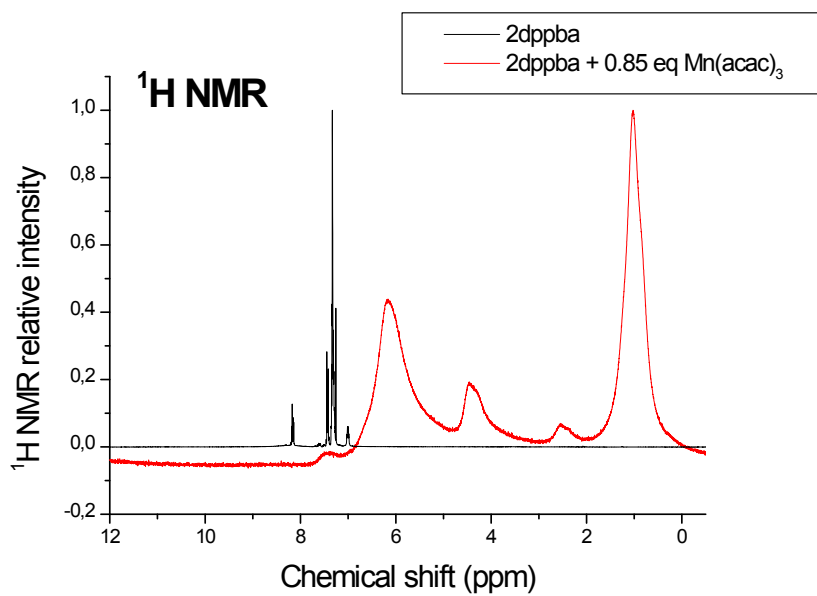


Figure S3. ¹H and ³¹P NMR in CDCl₃ of 7 mM 2dppba before and after adding 0.85 eq Mn(acac)₃

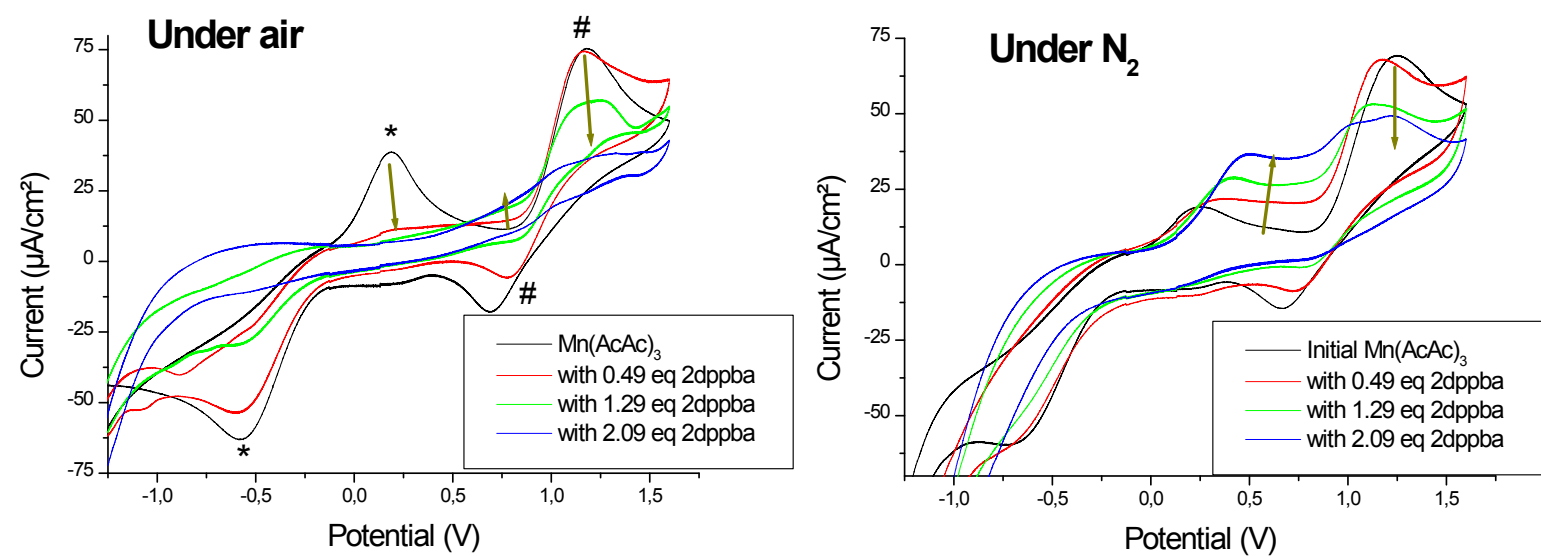
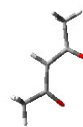
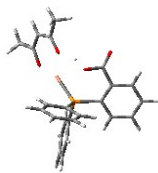
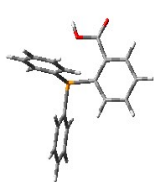


Figure S4. Cyclic voltammograms in ACN of 1.3 mM Mn(acac)₃ and increasing molar equivalent of 2dppba (following arrows). Under air (left) and under nitrogen saturated media (right, N₂). *:Mn(II)/Mn(III); #: Mn(III)/Mn(IV)

$$\Delta H = 37.17 \text{ kcal.mol}^{-1}$$



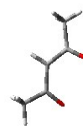
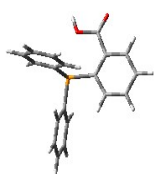
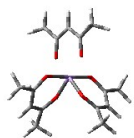
E = -886.55087 Ha

E = -889.86407 Ha

E = -1431.26649 Ha

E = -345.08922 Ha

$$\Delta H = 33.01 \text{ kcal.mol}^{-1}$$



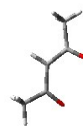
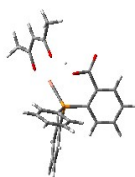
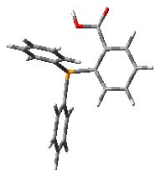
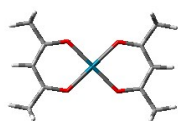
E = -1139.50222 Ha

E = -889.86407 Ha

E = -1684.22447 Ha

E = -345.08922 Ha

$$\Delta H = 57.42 \text{ kcal.mol}^{-1}$$



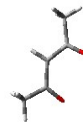
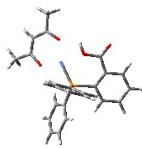
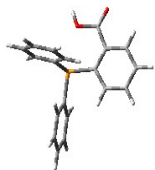
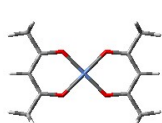
E = -817.12332 Ha

E = -889.86407 Ha

E = -1361.80667 Ha

E = -345.08922 Ha

$$\Delta H = 53.42 \text{ kcal.mol}^{-1}$$



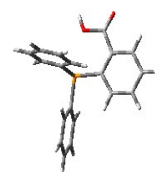
E = -859.72964 Ha

E = -889.86407 Ha

E = -1404.41936 Ha

E = -345.08922 Ha

$$\Delta H = 48.59 \text{ kcal.mol}^{-1}$$



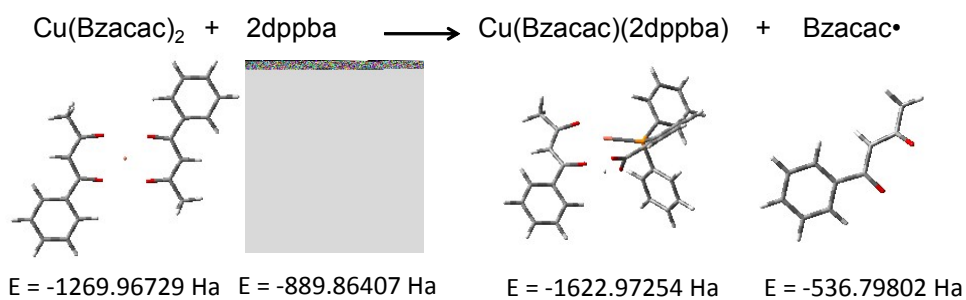
E = -1159.04812 Ha

E = -889.86407 Ha

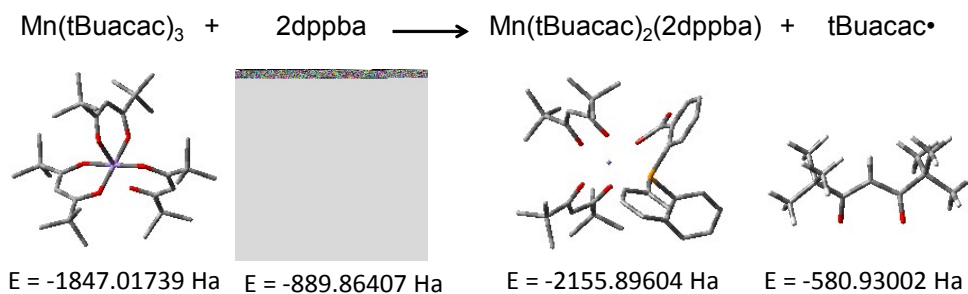
E = -1703.74554 Ha

E = -345.08922 Ha

$\Delta H = 38.15 \text{ kcal.mol}^{-1}$

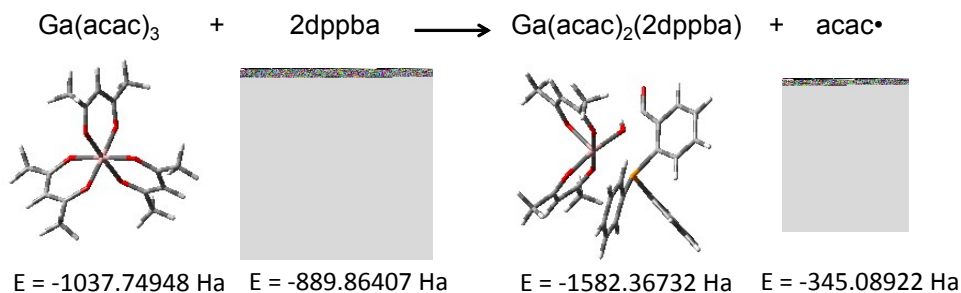


$\Delta H = 34.76 \text{ kcal.mol}^{-1}$

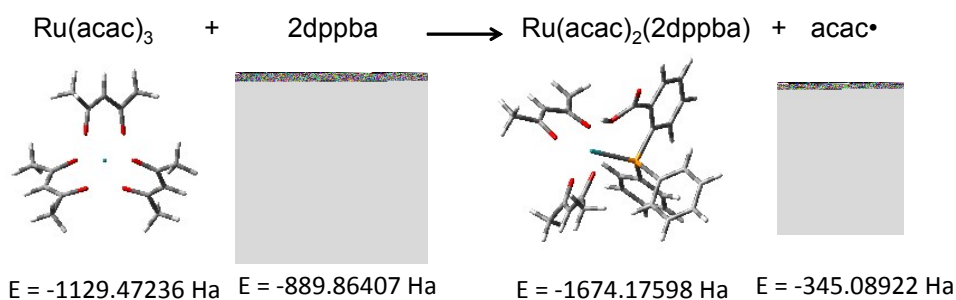


Note: hydrogens masked for both manganese complexes

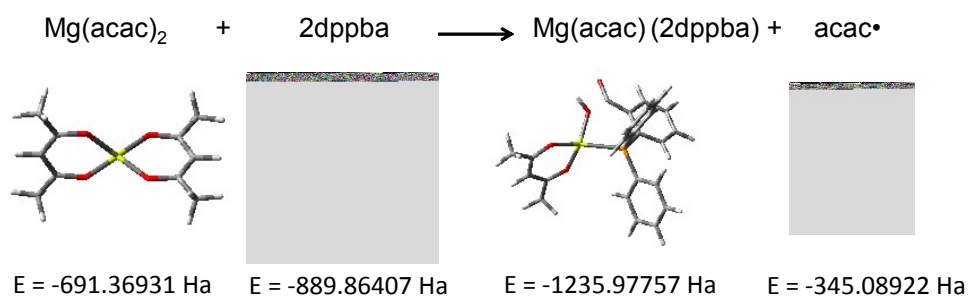
$\Delta H = 98.53 \text{ kcal.mol}^{-1}$



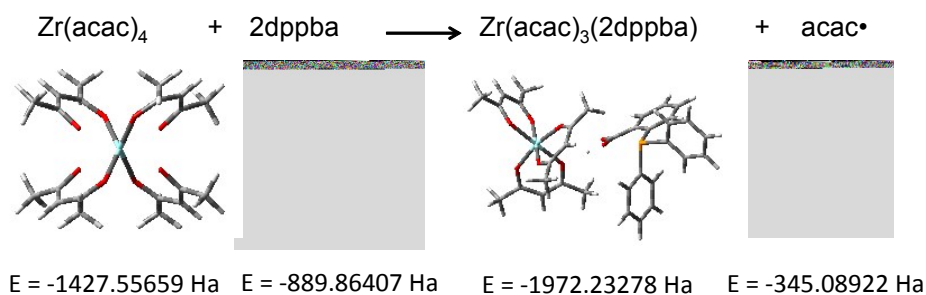
$\Delta H = 44.70 \text{ kcal.mol}^{-1}$



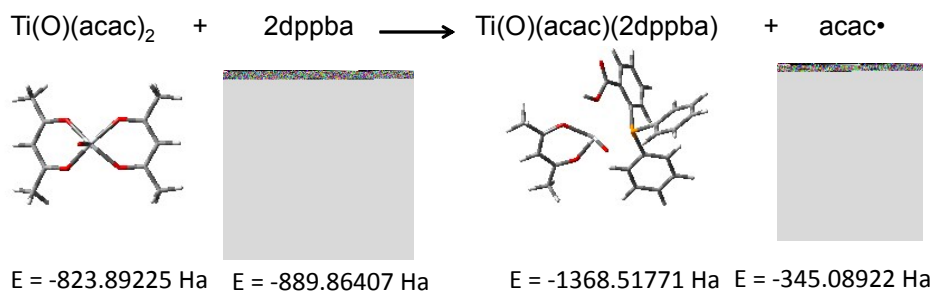
$\Delta H = 104.54 \text{ kcal.mol}^{-1}$



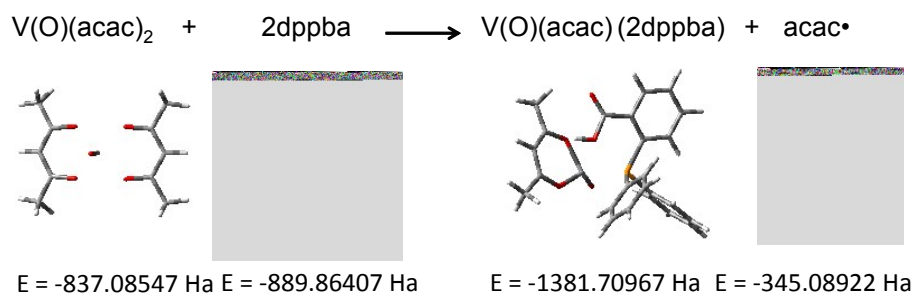
$\Delta H = 61.91 \text{ kcal.mol}^{-1}$



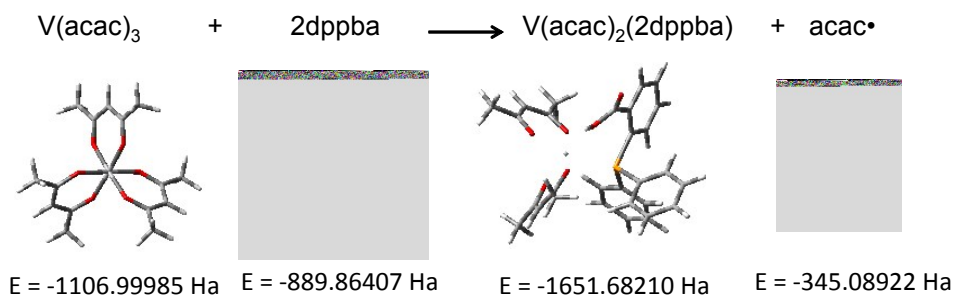
$\Delta H = 93.74 \text{ kcal.mol}^{-1}$



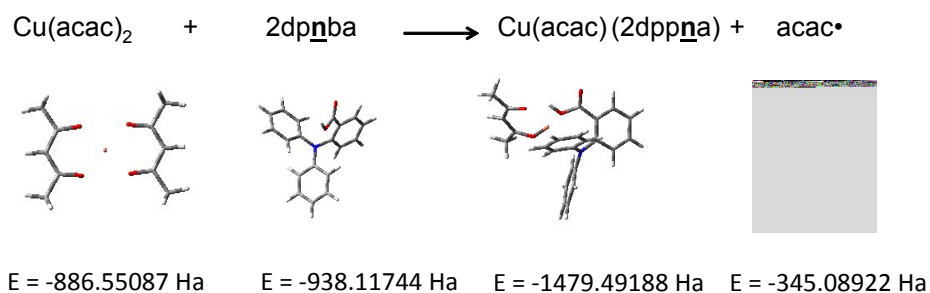
$\Delta H = 94.53 \text{ kcal.mol}^{-1}$



$\Delta H = 58.11 \text{ kcal.mol}^{-1}$



$\Delta H = 54.73 \text{ kcal.mol}^{-1}$



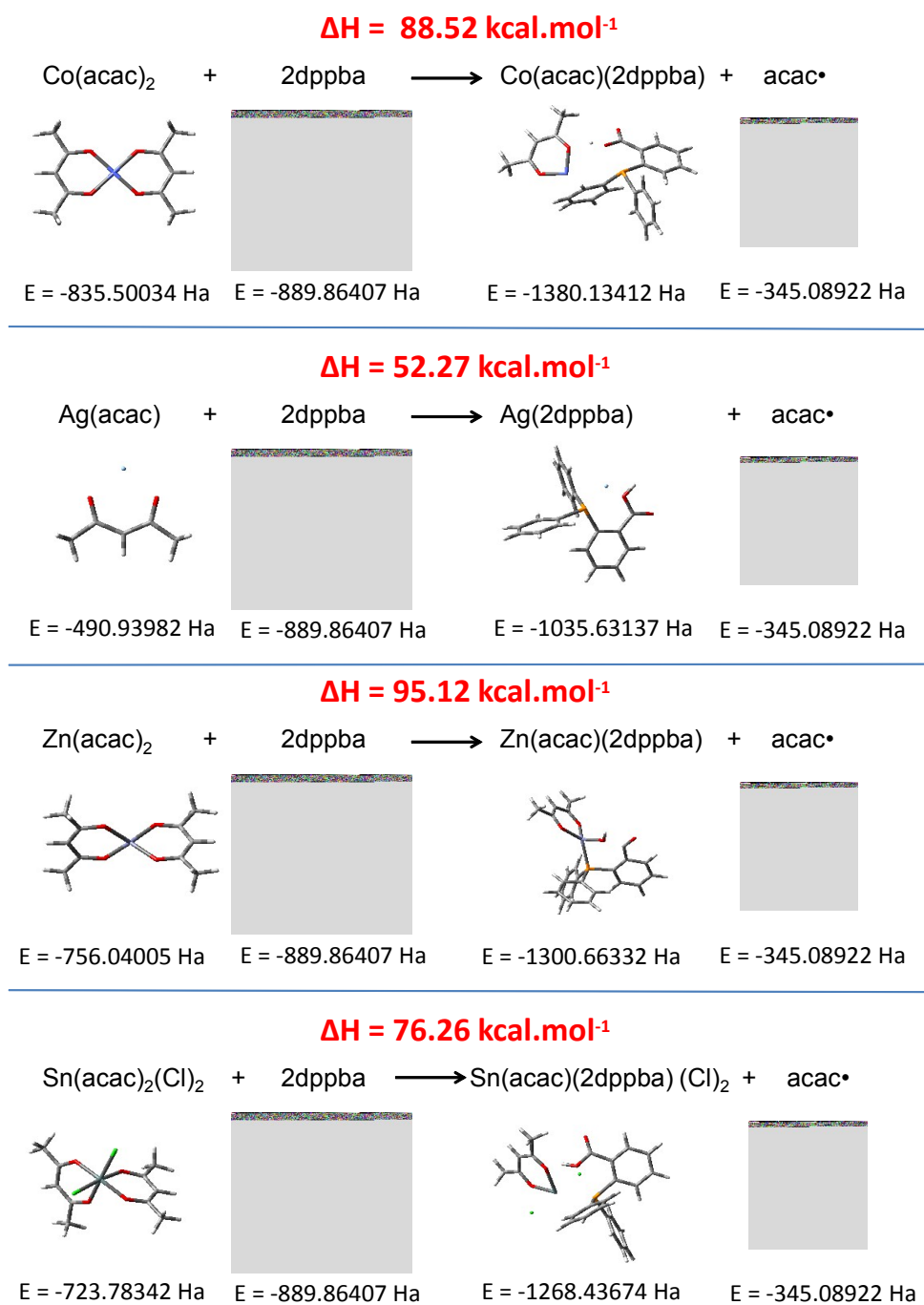
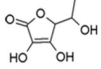
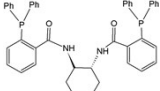
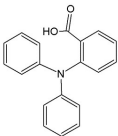
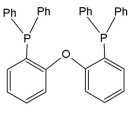
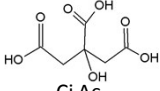
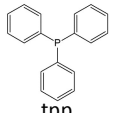
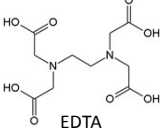
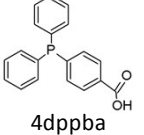
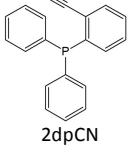


Figure S5. Optimized structures and reaction enthalpies of the MABLI reactions for various Metal acetylacetonates reacting with 2dppba (or 2dppnba in one case). Computed at UB3LYP/LANL2DZ level.

Table S2: Methacrylate polymerization according to the ligand/reducing agent used in combination with metal acetylacetonates.

entry	resin	ligand or reducing agent	quantity (wt%)	E_{ox}^a (V vs SCE)	Metal acac ^b (quantity)	Polymerization exothermicity ^{c,d}
1	1	 As Ac	1.5	0.72	Mn (1 wt%)	n.p
2	1	 Acet Ac	1.5	0.79	Mn (1 wt%)	n.p
3	1	 trost	1.5	0.93	Mn or Cu (1 wt%)	n.p
4	1	trost + Acet Ac	0.7 + 0.7	-	Mn (1 wt%)	n.p
5	1	trost + 4dppba	0.7 + 0.7	-	Mn (1 wt%)	n.p
6	1	 2dpnba	1.5	0.99	Cu (1 wt%)	n.p
7	1	2dpnba	1.5	0.99	Mn (1 wt%)	n.p
8	2	2dpnba	1.5	0.99	Mn (1 wt%)	n.p
9	1	 DPEphos	1.5	1.08	Mn or Cu (1 wt%)	n.p
10	1	 Ci Ac	1.5	1.10	Mn (1 wt%)	n.p
11	1	 tpp	1.5	1.25	Mn or Cu (1 wt%)	n.p
12	1	 EDTA	2	1.25 ¹⁴	Mn (1 wt%)	n.p
13	1	 4dppba	1.5	1.30	Mn or Cu (1 wt%)	n.p
14	1	 2dpCN	1.5	1.41	Mn or Cu (1 wt%)	n.p

^a: E_{ox} for half-wave reduction potential; ^b: Mn is Mn(acac)₃; Cu is Cu(acac)₂; Vac is V(acac)₃; Vox is V(O)(acac)₂; Mn or Cu stands for attempts with both metals separately; ^c: Room temperature=22±1 °C; 4mm sample; under air; polymerization curves in Figure S6 ^d: n.p for no polymerization

Table S3: Relationship between radical generation efficiency (for each metal acetylacetonate) and calculated data (ΔH of r1 and Mt-O distance in the initial metal acetylacetonate). Computed at UB3LYP/LANL2DZ level.



Mt(acac) _x	Efficiency of acac• release with 2dppba ^a	ΔH calculated (kcal.mol ⁻¹)	Mt-O distance calculated ^b (Å)
Ru(acac) ₃	no	44.70	1X 2.03 & 1X 2.04 & 1X 2.06
Fe(acac) ₃	no	48.59	2X 1.92 & 1X 1.93
Ag(acac)	no	52.27	1X 2.21
Ni(acac) ₂	no	53.42	2X 1.87
Pd(acac) ₂	no	57.42	2X 2.03
Zr(acac) ₄	no	61.91	2X 2.15 & 2X 2.27
Sn(acac) ₂ (Cl) ₂	no	76.26	1X 2.05 1X 2.07
Co(acac) ₂	no	88.52	2X 1.88
Ti(O)(acac) ₂	no	93.74	2X 2.00
Zn(acac) ₂	no	95.12	2X 1.98
Ga(acac) ₃	no	98.53	3X 1.95
Mg(acac) ₂	no	104.54	2X 1.94
Cr(acac) ₃	no	n.c ^e	n.c ^e

^a: estimated from the FRP initiation efficiency of methacrylate resins; ^b Mt-O for the acetylacetonate ligands: 1X stands for one acetylacetonate ligand when 2X or 3X stands for two or three ligands, respectively.; ^c: tBuacac• released; ^d: Bzacac• released; ^e: n.c: not calculated as Cr is not available in LANL2DZ package.

Table S3-bis: Example of Mt-O distance in the initial metal acetylacetonate found in the literature

Mt(acac) _x	Mt-O distance calculated ^b (Å)	Calculation or experimental method
Cu(acac) ₂ ¹⁵	2X 1.91-1.94	DFT study
Mn(acac) ₃ ¹⁶	1X 1.95 and 2X 2.0	XRD
Pd(acac) ₂ ¹⁷	2X 1.98	XRD
Ni(acac) ₂ ¹⁸	2X 2.08	XRD
Fe(acac) ₃ ¹⁹	distorted octahedron (> 1.99)	XRD
Co(acac) ₂ ²⁰	1X 2.01 and 1X 2.04	XRD

Table S4: Methacrylate polymerization according to the metal/oxidizing agent used in combination with 2dppba.

Oxidizing agent or Metal complexe + 2dppba \longrightarrow FRP ? (r2)

entry	resin	metal or oxidizing agent	quantity (wt%)	E _{red} (V vs SCE)	2dppba quantity (wt%)	Polymerization exothermicity
1	1	tBu-PBZ	1.50	0.18	1.5	n.p
2	1	CumOOH	1.50	0.08	1.5	n.p

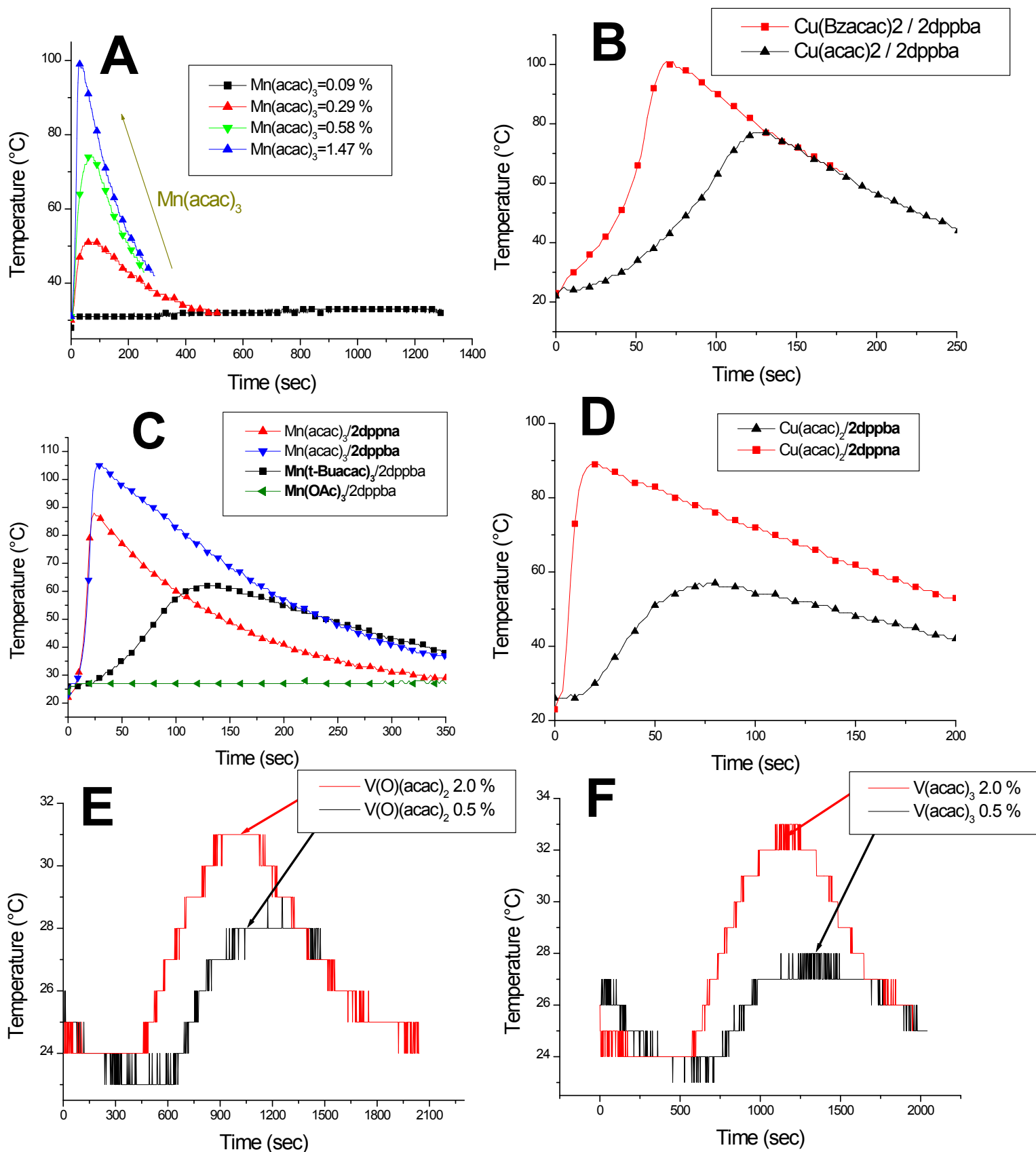


Figure S6 Optical pyrometric measurements during polymerization of **resin 1** (A, B, E, F) and **resin 2** (C, D) under air, 4 mm thick samples. **A:** for **2dppba**= 0.8 wt% mixed with increasing Mn(acac)₃ concentration. **B:** for **2dppba**= 1.5 wt% mixed with 0.7 wt% Cu(acac)₂ and 0.7 wt% Cu(Bzacac)₂. **C:** Optical pyrometric measurements during polymerization of **resin 2** under air with [Mn species] = 0.7 wt% and [2dppba or 2dppna] = 0.9 wt%. Comparison between initiating systems: Mn(acac)₃/2dppna

(□); Mn(acac)₃ /2dppba (■); Mn(t-Buacac)₃ /2dppba (▼); Mn(OAc)₃ /2dppba (◀).**D**: Comparison between initiating systems: Cu(acac)₂ =0.25 % / 2dppba = 0.65 % (□); Cu(acac)₂ = 0.25 % / 2dppna = 0.65 % (■).**E, F**: 1.5 wt% 2dppba mixed with: **E**: 0.5 wt% V(O)(acac)₂ and 2.0 wt% V(O)(acac)₂ **F**: 0.5 wt% V(acac)₃ and 2.0 wt% V(acac)₃

Table S5: HR-ESI-MS data. For two ligand exchanges: experiments 1-1; 1-2 and 1-3: V(O)(acac)₂ + 10 eq 2dppba and experiments 2-1,2-2 and 2-3: Mn(acac)₃ + 2 eq 2dppba. (error compared to theoretical masses, see Table S1)

Experiment	m/z experimental (Da)	Error (mDa)	Error (ppm)
1-1	472.0632	- 0.7	- 1.5
1-2	472.0634	- 0.5	- 1.1
1-3	472.0630	- 0.9	- 1.9
2-1	476.058	0	0
2-1	698.0817	+0.3	+0.4
2-2	476.0581	+ 0.1	+0.2
2-2	698.0817	+0.3	+0.4
2-3	476.059	+ 1.0	+2.1
2-3	698.0827	+1.3	+1.9

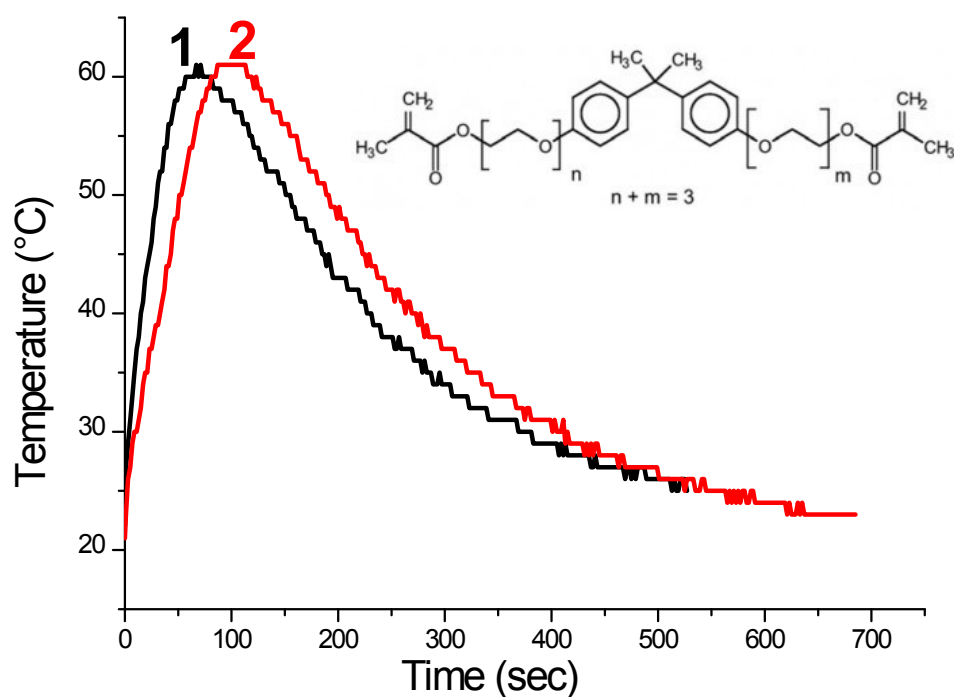


Figure S7: Optical pyrometric measurements (Temperature vs. mixing time) during polymerization in resin embedded (OH-free methacrylate resin, Aldrich) for **2dppba= 1.7 wt%** mixed 1.0 wt% Cu(acac)₂. **1:** initial formulation; **2:** after 15 days storage of both components at room temperature, under air.

Table S6: HR-ESI-MS data and proposed structural interpretation for 2dppba stability in methanol, under air (solution of about 4 mg/L 2dppba, stored 24 hours).

Detected (HR-ESI-MS) [M+H] ⁺	m/z (Da)	Error	Proposed attribution
C₁₉H₁₄O₂P⁺	305.0726	< 1 ppm	2-dppba
C₁₉H₁₆O₃P⁺	323.0832	< 3 ppm	2-dppba-ox
C₂₀H₁₈O₃P⁺	337.0988	< 2 ppm	2-dppba-ox esterificated

References:

- 1 K. L. Krishnakumar and R. Manju, *Int. J. Pharm. Sci. Res.*, 2013, **4**, 392.
- 2 S. K. Dey, B. Bag, Z. Zhou, A. S. C. Chan and S. Mitra, *Inorganica Chim. Acta*, 2004, **357**, 1991–1996.
- 3 B. Li, J. Lang, S. Wang and Y. Zhang, *J. Chem. Crystallogr.*, 2005, **35**, 547–550.
- 4 F. Gonçalves, Y. Kawano, C. Pfeifer, J. W. Stansbury and R. R. Braga, *Eur. J. Oral Sci.*, 2009, **117**, 442–446.
- 5 B. Falk, S. M. Vallinas and J. V. Crivello, *J. Polym. Sci. Part Polym. Chem.*, 2003, **41**, 579–596.
- 6 J. V. Crivello and J. H. W. Lam, *J. Polym. Sci. Polym. Chem. Ed.*, 1981, **19**, 539–548.
- 7 N. J. Everall, *Appl. Spectrosc.*, 2000, **54**, 773–782.
- 8 N. J. Everall, *Analyst*, 2010, **135**, 2512–2522.
- 9 W. S. Shin, X. F. Li, B. Schwartz, S. L. Wunder and G. R. Baran, *Dent. Mater.*, 1993, **9**, 317–324.
- 10 F. Courtecuisse, C. Dietlin, C. Croutxé-Barghorn and L. G. J. Van Der Ven, *Appl. Spectrosc.*, 2011, **65**, 1126–1132.
- 11 P. Garra, F. Dumur, D. Gignes, A. Al Mousawi, F. Morlet-Savary, C. Dietlin, J. P. Fouassier and J. Lalevée, *Macromolecules*, 2017, **50**, 3761–3771.
- 12 P. Xiao, F. Dumur, J. Zhang, J. P. Fouassier, D. Gignes and J. Lalevée, *Macromolecules*, 2014, **47**, 3837–3844.
- 13 J. Foresman and E. Frish, *Gaussian Inc Pittsbg. USA*.
- 14 J. Yang, X. Hu and J. Zhang, *J. Hazard. Mater.*, 2010, **181**, 742–746.
- 15 M. Bruschi, L. D. Gioia, R. Mitrić, V. Bonačić-Koutecký and P. Fantucci, *Phys. Chem. Chem. Phys.*, 2008, **10**, 4573–4583.
- 16 A. A. Dakhel, *Mater. Chem. Phys.*, 2006, **96**, 422–426.
- 17 S. H. Mushrif, A. D. Rey and G. H. Peslherbe, *Chem. Phys. Lett.*, 2008, **465**, 63–66.
- 18 G. J. Bullen, R. Mason and P. Pauling, *Inorg. Chem.*, 1965, **4**, 456–462.
- 19 M.-L. Hu, Z.-M. Jin, Q. Miao and L.-P. Fang, 2001, 597–598.
- 20 V. D. Vreshch, J.-H. Yang, H. Zhang, A. S. Filatov and E. V. Dikarev, *Inorg. Chem.*, 2010, **49**, 8430–8434.